Eur Biophys J (1999) 28: 269–278

ARTICLE

A. Bjørkøy · A. Mikkelsen · A. Elgsaeter

Transient electric birefringence of human erythroid spectrin dimers and tetramers at ionic strengths of 4 mM and 53 mM

Received: 26 August 1998 / Revised version: 8 February 1999 / Accepted: 11 February 1999

Abstract In conventional electrooptic studies the sample ionic strength must for technical reasons be kept below about 3 mM, which is only 2% of the ionic strength at physiological conditions. In particular for flexible polyelectrolytic macromolecules it can in general not be ruled out that both the conformational average and dynamics at ionic strength 3 mM and below may differ significantly from what it is at physiological conditions. Here we report on the first electrooptic study of human erythroid spectrin dimers and tetramers at ionic strengths higher than 3 mM. All measurements in this study were carried out at both ionic strength 4 mM (2.5 mM HEPES + 1 mM NaCl) and 53 mM (2.5 mM HEPES + 50 mM NaCl). Spectrin tetramers were studied only at 4 °C whereas the dimers were studied at both 4 °C and 37 °C. At 4 °C there is a striking quantitative similarity between the transient electric birefringence (TEB) of spectrin dimers and tetramers. Also, the TEB of spectrin dimers at 37 °C was very similar to the results at 4 °C. The contour length and the molecular weight of spectrin dimers and tetramers are known. The dominating TEB relaxation time is in all cases only a fraction of what is predicted theoretically if the spectrin dimers and tetramers are assumed to be stiff and extended molecules. In sum, the new TEB data constitute strong electrooptic evidence confirming that spectrin dimers and tetramers have a highly flexible structure, and demonstrate for the first time that a major part of the intrachain dynamics of the spectrin is quite insensitive to an increase of the ionic strength from 4 mM to 53 mM. Use of the reversing electric field pulse technique for all conditions studied yields TEB data suggesting that the orientation of both spectrin dimers and tetramers in an electric field is dominated by a permanent rather than an induced electric dipole moment.

A. Bjørkøy · A. Mikkelsen · A. Elgsaeter (✉)
Norwegian University of Science and Technology (NTNU),
Norwegian Biopolymer Laboratory (NOBIPOL),
Department of Physics, Sem Saelandsvei 9,
N-7491 Trondheim, Norway
e-mail: arnelg@phys.ntnu.no

Key words Spectrin · Birefringence · Rotational relaxation · Intrachain conformational relaxation

Abbreviations *EDTA* Ethylenediaminetetraacetic acid · *HEPES* *N*-(2-Hydroxyethyl)piperazine-*N′*-(2-ethanesulfonic acid) · *HPIB-bus* Hewlett-Packard Interface Bus · *MOSFET* Metal oxide semiconductor field-effect transistor · *SDS* Sodium dodecyl sulfate · *TEB* Transient electric birefringence · *Tris* Trimethamine · *TTL* Transistor-transistor logic

Introduction

Erythrocyte shape and strength are to a large extent determined by a submembrane network, or membrane skeleton, whose major component is erythroid spectrin. A spectrin dimer is composed of one elongated α-chain and one β-chain aligned in an antiparallel manner and interconnected at each end. Human erythrocyte spectrin dimers as visualized by standard transmission electron microscopy appear to be flexible with loosely intertwined subchains and to have a contour length of about 100 nm, a diameter of 4–6 nm and a persistence length of 16–20 nm (Shotton et al. 1979; Stokke et al. 1985). Spectrin is stabilized and anchored to the plasma membrane by other accessory proteins (Bennett and Lambert 1991). The spectrin α-chains and β-chains are composed of 19 and 21 homologous segments, respectively, linked in tandem. With only a few exceptions, each segment consists of 106 amino acids (Speicher and Marchesi 1984) that make up a compact triple-helical bundle (Yan et al. 1993; Pascual et al. 1997). Each segment is connected to its topological neighbour by a flexible link. At pH 7.6 and ionic strength 1 mM the net charge per dimer is –65, while at ionic strength 50 mM and the same pH the net charge equals –45 (Elgsaeter et al. 1976).

Head-to-head association of two dimers yields a tetramer, which is the prevailing oligomeric form of spectrin in the native erythrocyte skeleton (Begg et al. 1994). Spec-

trin extraction at low ionic strength from erythrocyte membranes (ghosts) can yield both dimers and tetramers. In solution, the dimer-tetramer equilibrium depends on both temperature and ionic strength (Ungewickell and Gratzer 1978; Ralston 1991; Cole and Ralston 1992; Henniker and Ralston 1994). The contour length of the spectrin tetramer is about 200 nm.

The erythrocyte's capacity to withstand environmental changes, and to deform and contract during growth and development, can in part be explained by spectrin's flexibility within the membrane anchored network (Elgsaeter et al. 1986; Goodman et al. 1988; Bennett 1990; Dhermy 1991; Elgsaeter and Mikkelsen 1991). The intrachain dynamics of spectrin has primarily been studied by measuring electron paramagnetic resonance of labelled spectrin molecules (Fung and Johnson 1983), nuclear magnetic resonance (Fung et al. 1986; Begg et al. 1994) and transient electric birefringence (TEB) (Mikkelsen and Elgsaeter 1978, 1981; Roux and Cassoly 1982). These data all indicate that the spectrin chains undergo major thermally induced conformational changes both when they are free in solution and in situ, i.e. integrated in the membrane skeleton.

Data available in the literature on the effective hydrodynamic radius (Ralston and Dunbar 1979), intrinsic viscosity (Stokke et al. 1985) and the radius of gyration (Elgsaeter 1978) for isolated spectrin reveal a significant increase in these parameters when the ionic strength is reduced. These results suggest that the intrachain electrostatic interactions of the flexible and highly charged spectrin molecules have a significant effect on the average equilibrium conformation at low ionic strength. The reported TEB studies of human erythrocyte spectrin were carried out at ionic strength 3 mM, or less, i.e. at an ionic strength that is less that 2% of the ionic strength corresponding to physiological conditions. It could therefore not be ruled out that the intrachain dynamics for the ionic strength conditions used in the earlier TEB studies might differ significantly from the dynamics at physiological conditions.

Here we report on the first TEB study of isolated human erythroid spectrin dimers and tetramers at ionic strength above 3 mM. The new measurements were carried out at ionic strengths 4 mM and 53 mM in order to elucidate to what extent the intrachain conformational dynamics of these flexible and highly charged proteins is ionic strength dependent. For reasons not yet understood, we obtained a significant (±15%) systematic difference in the parameter estimates obtained using spectrin isolated and purified from separate standard hospital blood bags. Because of this we will only present a semi-quantitative discussion of the new spectrin TEB data.

Materials and methods

High current and high voltage pulse generator

To carry out the study presented here we designed, built and tested an all-solid-state high current (max 90 A) and high voltage (max 4 kV) pulse generator. The electric pulse rise and decay times are 12–25 ns and 45–85 ns, respectivley (for details see at end of this section). The pulse length can be varied from 1 µs to 10 ms. The pulse generator delivers both single pulses and reversing double pulses consisting of one positive pulse followed within less than 100 ns by a negative pulse. The shortest repeat time between individual single or reversing double pulses is 2–10 s, depending on the pulse voltage.

The main technological development that made the design of the new pulser possible was the availability of the new metal oxide semiconductor field-effect transistor (MOSFET) high current/high voltage switches manufactured by Behlke (Frankfurt, Germany). For our pulse generator we chose switch type HTS 81-09 which operates at a maximum of 8 kV and 90 A. The typical turn-on and turn-off times of these particular switches, according to the data supplied by the manufacturer, equal 30–35 ns. The switches are compact (178×64×27 mm) and can be turned ON/OFF using standard transistor-transistor logic (TTL) level signals. A simplified circuit diagram of our new high current/voltage pulser is shown in Fig. 1.

A single external TTL-level pulse from a personal computer triggers an internal TTL pulse generator which produces one pulse with length predetermined by four thumb wheels. The decimal number set by the thumb wheels specifies the pulse length in µs. If the circuitry is preset to generate reversing high voltage double pulses, the output from the first internal TTL pulse generator is used to trigger a second internal TTL pulse generator which is identical to the former.

To obtain a robust design it is important to protect the HTS 81-09 solid state switches against overload. It is in particular important that the switch controlling the first pulse is turned fully off before the switch controlling the second reversed pulse is turned on. To secure this, a selectable time delay has been added between the first internal TTL pulse generator and the associated high current and high voltage switch. The delay can be changed in steps of 20 ns. It may not be advisable to use delays that are shorter than 100 ns even though this is technically fully possible. To further protect the HTS 81-09 switches, resistors R_S have been added to function as current limiters. Components C_D and R_D provide protection against high voltage spikes caused by the inductive part of the load. The values of these components are changed depending on whether the pulse generator operates in the single pulse or the reversing pulse mode (not shown). As an additional protective measure the amplitude of the generated reversing pulses have been limited to a maximum of 4 kV.

As our high voltage source we use two Bertran (Hicksville, USA) 800 high voltage supplies (5 kV, 10 mA). The two electrolyte capacitors C_{HT} (Fig. 1) each consists of three 4 µF (max 6.3 kV) Siemens (Germany) capacitors coupled in parallel. With a load resistance of 50 Ω the inherent build-up time of the capacitor voltage, and thus the voltage across the Kerr cell, equals 25 ms. The capacitors used are low-inductance capacitors designed especially to deliver short high-current pulses. The current

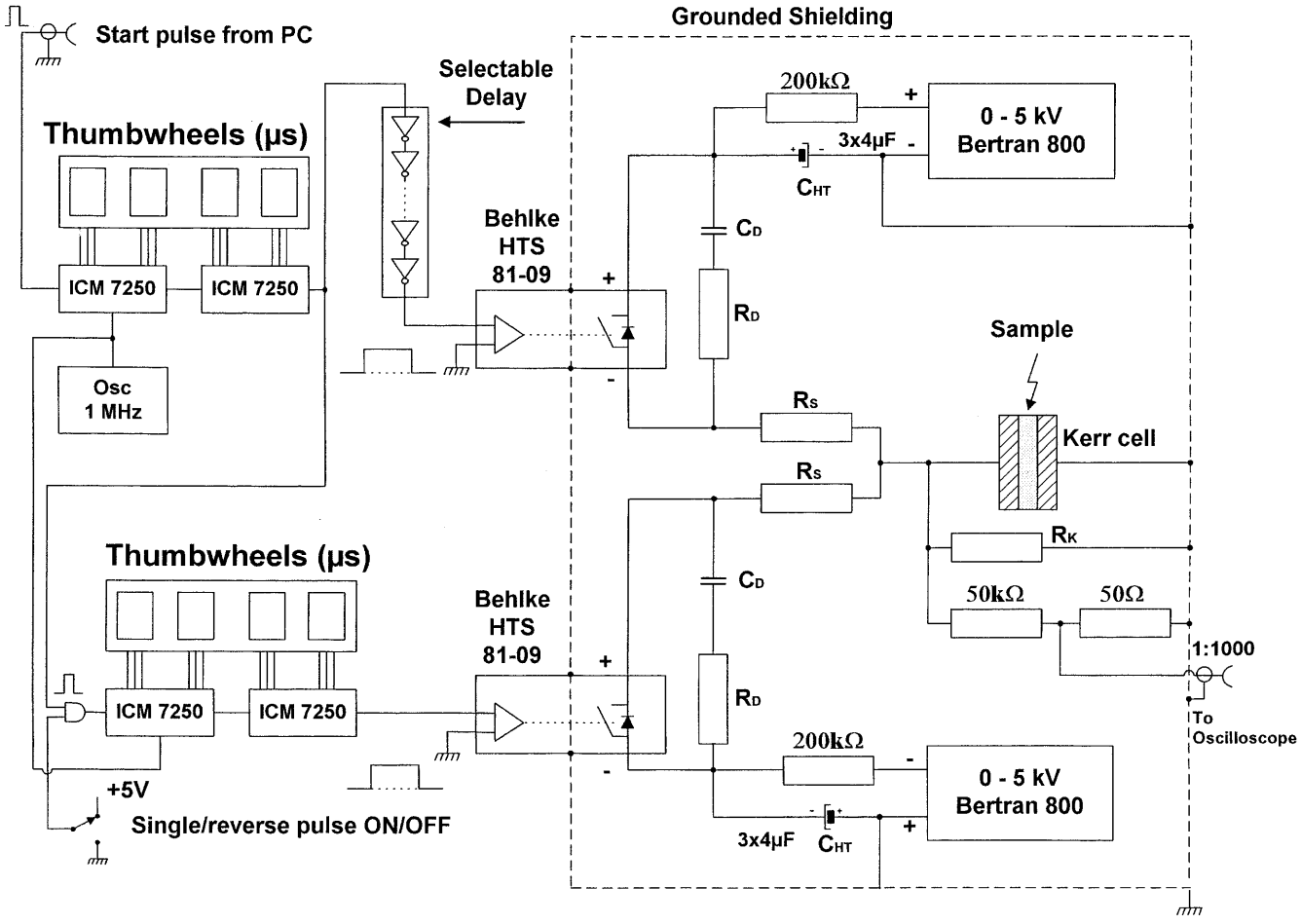

Fig. 1 Simplified circuit diagram of our new, all solid state, high current (max 90 A) and high voltage (max 4 kV) pulse generator. The pulser can produce single pulses or symmetric, reversing electric double pulses. The delay between the first (positive) and second (negative) pulse is selectable in steps of 20 ns. The Kerr cell voltage is monitored by an oscilloscope through a 1:1000 voltage divider in parallel with the selectable load resistor R_k and the Kerr cell

change through the Kerr cell can be as high as 3×10^9 A/s. Great care was therefore taken to keep all leads carrying high current as short as possible and to make sure that there is adequate electrostatic shielding between the compartments containing the high current circuits and the compartments containing TTL circuitry.

We found that both the rise time and the decay time of the pulses depend on the resistance of the external load. Therefore, a selectable resistor R_k in parallel with the Kerr cell (Fig. 1) was included in order to minimize the decay times of the electric pulse when samples with high electric impedance were studied. Using resistor R_k equal to 50 Ω and 180 Ω, we found the pulse rise time to be 25 ns and 12 ns, respectively. For R_k equal to 50, 180 and 540 Ω we found the pulse decay time to be 45, 80 and 85 ns, respectively. For more technical details, see Bjørkøy (1997).

Preparation of human erythroid spectrin dimers and tetramers

Spectrin was obtained from outdated human blood (Sagman blood) kindly provided by the Trondheim Regional Hospital. Unless otherwise stated, all the preparation steps were carried out at 0–4 °C and pH 7.6. A sample containing 80–100 ml Sagman blood was washed twice in 600 ml 310 mosM phosphate buffer. The packed erythrocytes were lysed by adding the cells to 900 ml of 20 mosM phosphate buffer and left stirring for 15 min. Next 300 ml of this ghost suspension was harvested by centrifugation at 17 000 rev/min in a Beckman (Palo Alto, California, USA) Ja-17 rotor for 30 min and resuspended in 300 ml of 2 mosM phosphate buffer and 9 mM NaCl, followed by centrifugation at 17 000 rev/min for 30 min. The remaining 2×300 ml of ghost suspension were processed as described above. The ghosts from the three parallels were pooled and resuspended in 300 ml of 2 mosM phosphate buffer and 9 mM NaCl.

Spectrin was extracted by dialysing the ghosts for 48–62 h against 3×1000 ml 0.1 mM EDTA and 0.05 mM dithiothreitol at pH 9.5. The suspension of ghosts was centrifuged at 50 000 rev/min in a Beckman 50Ti rotor for 60 min. The supernatant containing the crude ghost extract was applied to a 450×26 mm gel filtration column (col-

umn one) containing Sepharose CL-4B beads (Pharmacia, Uppsala, Sweden) equilibrated with 0.1 mM EDTA, 0.05 mM dithiotreitol and 1 mM Tris-HCl (pH 8.0), partly in order to remove actin and residual hemoglobin, but mainly to remove small amounts of proteases normally present in the crude extracts. The column was eluted at a flow rate of 15 ml/h. The spectrin contents of the various fractions from the column were determined by measuring the absorbance at 280 nm. The eluted spectrin was mainly in the tetrameric form. One half of the spectrin-containing peak was incubated at 37 °C for 30 min, resulting in nearly 100% conversion to dimers. It is important that no active protease is present during this step of the procedure. After cooling to 0–4 °C the spectrin dimer solution was applied to a 900×16 mm gel filtration column (column two) containing Sepharose CL-4B beads equilibrated with 100 mM NaCl, 0.1 mM EDTA and 0.05 mM dithiothreitol (pH 7.4). The column was eluted at a flow-rate of 10 ml/h and the spectrin fractions were analysed as described above.

The rest of the spectrin dimer-tetramer fraction from column one was applied to column two and eluted with the same eluent buffer and the same flow rate as described above. This yielded a dominant spectrin tetramer and a minor spectrin dimer containing peak. Only the spectrin tetramer fraction from this column was used. The obtained spectrin dimer and tetramer fractions were concentrated as needed by vacuum dialysis (Micro-ProDiCon, Spectrum, USA) against 2×1000 ml of 2.5 mM HEPES and 1 mM NaCl (pH 7.5) for 24–30 h. For some of the samples, the final NaCl concentration was adjusted to 50 mM. Hence the ionic strengths of the samples were either 4 mM or 53 mM. The concentration of dimers and tetramers was 0.25 mg/ml in the 1 mM NaCl buffer and 0.5 mg/ml in the 50 mM NaCl buffer (except for the dimer samples from preparation 1, which had a concentration of 0.25 mg/ml). The concentrations were determined by UV-light absorbance measurements using a specific absorbance of $A_{1\%}^{1\,\mathrm{cm}}$ (280 nm) = 10.1 (Elgsaeter 1978).

SDS polyacrylamide gel electrophoresis of some of the spectrin samples was carried out after all measurements of the particular sample had been completed in order to check whether any proteolytic degradation had taken place during the birefringence measurements. For all samples investigated, no significant amount of proteolytic products could be observed.

Measurement of TEB

The samples were placed in a Kerr cell with 13.8 mm optical path length and 4.0 mm electrode separation [for more technical details see Bjørkøy (1997)]. The spectrin dimer and tetramer samples were subjected to electric pulses of 50–150 µs and 100–250 µs duration, respectively. The pulses were generated using the new high current and high voltage solid state pulse generator described above, and the applied electric field strength ranged from 0.2 kV/cm to 1.5 kV/cm. The temperature of the Kerr cell was controlled by a Haake D8 Thermostat (Karlsruhe, Germany). The electric birefringence of spectrin dimers was measured at 4 °C and 37 °C, whereas the spectrin tetramers were measured at 4 °C only. The dimer samples were kept on ice until shortly before the birefringence measurements and the measurements for each sample lasted less than half an hour. From available kinetic data (Ungewickell and Gratzer 1978) it can be estimated that, for the spectrin dimer concentration used, less than about 10% will convert to tetramers within 30 min at 37 °C.

Included in the standard optical detection system (Fredericq and Houssier 1973) were an Omnichrome Argon laser (Chino, California, USA) model 543-AP operated at wavelength $\lambda = 488$ nm (polarized light), one half-wave plate, two polarizers (extinction coefficients equal 10^{-7}), one quarter-wave plate obtained from Halle (Berlin, Germany) and a photomultiplier type RCA 1P28 (EMI Electronics, Middlesex, England) operated at an anode voltage of about 630 V. The electric field vector of the incident polarized light beam was oriented 45° relative to the electric field across the Kerr cell. The measurements were carried out in the linear detection mode with the analyser rotated an angle 90° + 4.5° relative to the polarizer. The electric field pulse and the signal from the photomultiplier tube were displayed on a Tektronix TDS 620 digital storage oscilloscope (Beaverton, Oregon, USA) with 500 MHz bandwidth. Data stored in the oscilloscope were transferred by a Hewlett-Packard Interface Bus (HPIB-bus) communication line to a personal computer for further analysis. Details of the employed instrument are published elsewhere (Bjørkøy 1997; Bjørkøy et al. 1999a, b).

The temperature increase, ΔT, caused by the electric current that passes through the spectrin sample in the course of one electric field pulse of duration Δt and strength E, is given by the expression

$$\Delta T = \frac{(E\,l)^2}{c_\mathrm{p}\, m\, R_\mathrm{KC}}\,\Delta t \qquad (1)$$

where l is the electrode separation and R_KC the electric resistance of the Kerr cell, m is the mass and c_p the specific heat capacity of the sample. The resistance R_KC depends on the ionic composition of the sample, as well as on the Kerr cell dimensions. Inserting actual values used in our experiments into Eq. (1), we found that the temperature elevation did not exceed 1 °C per electric pulse, and could therefore be neglected.

Decay and rise times measured at other temperatures than 20 °C were scaled to 20 °C ($\tau^{(20)}$) using the standard temperature and viscosity conversion factor (Bjørkøy et al. 1999b). For example, for τ measured at 4 °C we employ the adjustment

$$\tau^{(20)}(4\,^\circ\mathrm{C}) = \frac{\eta(20\,^\circ\mathrm{C})/T(20\,^\circ\mathrm{C})}{\eta(4\,^\circ\mathrm{C})/T(4\,^\circ\mathrm{C})}\,\tau(4\,^\circ\mathrm{C}) \qquad (2)$$

where $\eta(T)$ is the solvent viscosity at the absolute temperature T.

In all experiments described we used aqueous solutions. For samples with very low spectrin concentration, the

electric induced birefringence of water itself may constitute a significant part of the total birefringence. However, we found that for the electric field strengths and spectrin concentrations employed in the work described here, the water birefringence signal could be neglected.

The rise and decay times of the new solid state high current and high voltage pulser is 10–100 times shorter than those of the pulsers used in previous birefringence studies of spectrin. The time resolution and the number of data points that can be stored using the current data acquisition system represent a 2–10 times improvement compared to the system used in the previous spectrin birefringence studies. For more technical details, see Bjørkøy (1997).

Results and discussion

Different sets of TEB data collected using the same spectrin sample produced highly reproducible parameter estimates (standard deviation less than 3–5%). However, we found that the relaxation time estimates obtained using data belonging to spectrin prepared from separate hospital blood bags showed a systematic shift as high as ±15% from the average values, which is much more than could be accounted for by stochastic noise alone. This was true both for spectrin dimers and tetramers. This variation may partly be caused by the fact that each blood bag originates from different individuals and/or may have been stored for different lengths of time. It is also possible that some minor proteolysis has passed undetected in the SDS gel analysis or that spectrin from the different sources has undergone different extents of dephosporylation or possibly deamination, but this still remains to be elucidated.

Partly because of these systematic shifts in the parameter estimates and partly because quantitative analysis of segmented polymers generally is a major task itself, we will here only present a semi-quantitative discussion of the new experimental data of spectrin birefringence. A detailed quantitative analysis of spectrin birefringence data which involves numerical Brownian dynamics simulation and use of the newly developed needle chain model (Nyland et al. 1996) and/or the needle-spring chain model (Mikkelsen et al. 1998) for segmented polymers is in progress. This work will presented in due course.

The TEB data of spectrin obtained using the current experimental set-up is in most aspects superior to data obtained by the equipment employed a decade ago. This is partly because of the great improvement represented by the characteristics of the new solid state electric pulse generator and in part because of the improved time resolution and the increased storage capacity of the high speed data acquisition system.

TEB of erythroid spectrin dimers

The specific stationary birefringence of spectrin dimers, $\Delta n_\infty/c$, at 4 °C as a function of λE^2 is shown in Fig. 2. Here

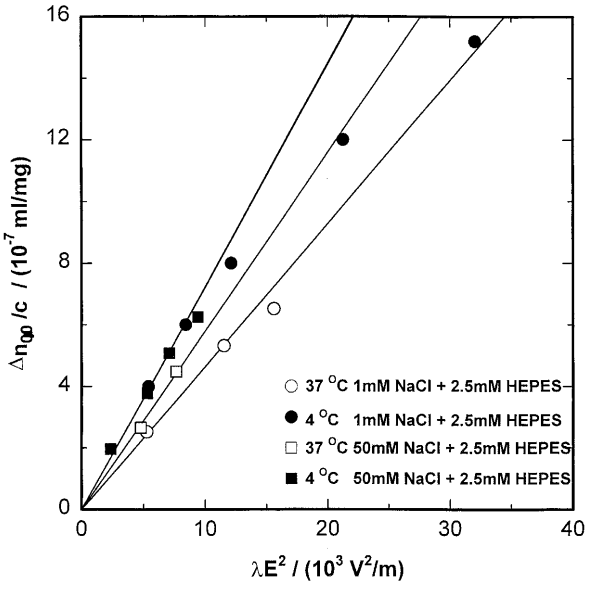

Fig. 2 Specific stationary birefringence $\Delta n_\infty/c$ for spectrin dimers as a function of λE^2 where c is the spectrin concentration in mg/ml, λ=488 nm is the wavelength of the light and E is the electric field strength across the Kerr cell. *Filled symbols* depict data obtained from spectrin dimer preparation 2, *open symbols* corresponds to data obtained from preparation 3 (Table 1). Measurements were carried out at pH 7.5 and the spectrin concentration was c=0.25 mg/ml (*circles*) and c=0.50 mg/ml (*squares*). The *solid lines* were obtained using linear regression

Δn_∞ is the stationary change in birefringence due to the applied electric field E. Parameter c is the spectrin concentration and λ is the wavelength of the laser light. A linear dependence of $\Delta n_\infty/c$ on E^2 was observed for low electric fields, but the birefringence deviated from the Kerr law at the highest electric field strengths employed. This was also reported in earlier spectrin studies (Mikkelsen and Elgsaeter 1978, 1981). Accurate estimation of the saturation birefringence value expected for very high electric field strength was not possible because the applied electric field strength was too low. The specific Kerr constant, B_s, equals the slope of each regression line in Fig. 2. Increasing the ionic strength from 4 mM to 53 mM resulted in a barely significant (less than 20%) increase in B_s, while increasing the temperature from 4 °C to 37 °C resulted in about 30% decrease in B_s. The average value for the regression lines presented in Fig. 2 is $B_s=(6\pm2)\times 10^{-11}$ m^4/(V^2 kg), which is in agreement with previous results (Mikkelsen and Elgsaeter 1978, 1981).

Figure 3 shows a representative plot of the spectrin dimer TEB at 4 °C and ionic strength 53 mM associated with application of one single rectangular electric pulse across the Kerr cell. A one-component exponential decay function can be adequately fitted to the TEB build-up data for the solution containing 50 mM NaCl, but for the solution containing 1 mM NaCl two exponentials were required. The TEB build-up data obtained for spectrin dimers could at low electric field strengths be fitted adequately using a one-component exponential function, but for

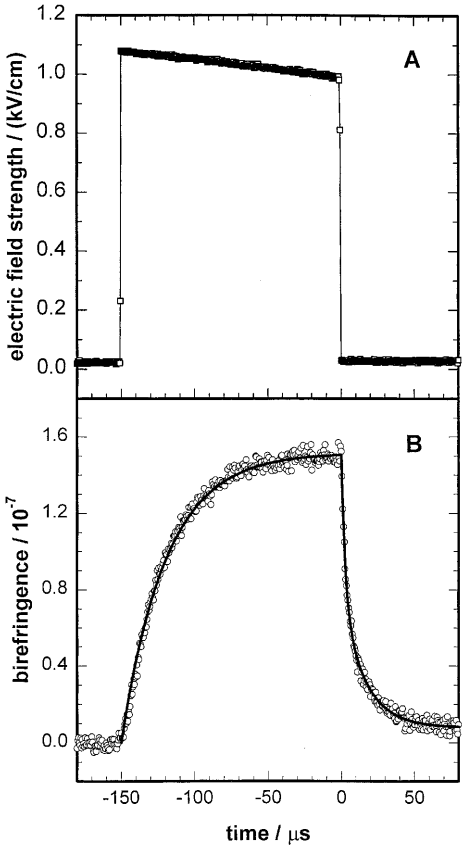

Fig. 3 **A** Electric field strength across the Kerr cell and **B** the resulting birefringence signal of spectrin dimer at 4 °C (preparation 3) in 2.5 mM HEPES and 50 mM NaCl at pH 7.5 (○). The spectrin dimer concentration was 0.5 mg/ml. Data points were recorded every 0.5 μs. The *solid lines* in **B** denote the best fit when a one-exponential function (build-up) or a two-exponential function (relaxation) was fitted to the experimental data using non-linear regression. The time constant for the birefringence build-up equals $\tau_r = 30.4 \pm 0.2$ μs and the two time constants for the free birefringence decay equal $\tau_{d,1} = 2.7 \pm 0.2$ μs (51%) and $\tau_{d,2} = 15.7 \pm 0.9$ μs (49%)

higher electric field strengths two exponentials were required. Details of the results from the analyses of the spectrin dimer TEB build-up and decay data are summarized in Table 1. All times presented in Table 1 are scaled to what is predicted at 20 °C by taking into account both the change in temperature itself and the temperature dependence of the water viscosity using Eq. (2). The two relaxation times at 4 °C averaged over all preparations were found to be 1.5 μs and 9.4 μs for both ionic strengths. The averaged single relaxation time at 37 °C was found to be 2.4 μs. The TEB rise times are significantly longer than the decay times, indicating that the spectrin dimer electric dipole moment is mainly permanent and not induced (Fredericq and Houssier 1973).

The parameter estimates presented in Table 1 differ somewhat from the values found in the literature (Mikkelsen and Elgsaeter 1978, 1981; Roux and Cassoly 1982). This is not surprising considering the differences in ionic strength used, electric field strength and that the estimates obtained using the older data in general are more uncertain. The estimates obtained are within the parameter range obtained using numerical simulations to predict the spectrin dimer rotational relaxation times (Skjetne et al. 1995). The experimental results reveal that increasing the NaCl concentration from 1 mM to 50 mM results in only minor changes in the TEB signal. This at first sight somewhat surprising result suggests that at these two ionic strengths the internal conformational dynamics of spectrin dimers which play a role in TEB is strikingly similar.

Figure 4 shows a representative example of the TEB signal when spectrin dimers at 37 °C in 1 mM NaCl + 2.5 mM HEPES were subjected to symmetric reversing electric field pulses. The minimum of the birefringence was found to be reached after a time ranging from 5.6 μs to 11.5 μs after sign reversal of the electric field, and the relative minimum values were in the range 0.02–0.2 for solutions at low ionic strength. For dimers in the 53 mM ionic

Table 1 Birefringence rise $\tau_r^{(20)}$ and decay $\tau_d^{(20)}$ times of erythroid spectrin dimers obtained at 4 °C and 37 °C, scaled to what is predicted at 20 °C using Eq. (2). The given time constants are the average values for electric field strengths of 0.2–1.5 kV/cm. The spectrin dimer concentration is 0.25 mg/ml in the 1 mM NaCl buffer and 0.5 mg/ml in the 50 mM NaCl buffer, except for the samples from preparation 1, which had a concentration of 0.25 mg/ml. When a two-exponential function is fitted to the experimental data, the two time constants are indicated by subscripts 1 and 2, and a relative amplitude is given for each. The uncertainties of the relaxation time estimates and the relative amplitudes are about ±10%, except for the amplitudes of $\tau_{r,1}^{(20)}$ and $\tau_{r,2}^{(20)}$ which have uncertainties of up to ±40%

Ionic strength	T (°C)	Prep. no.	Time constants (μs)					
			$\tau_r^{(20)}$	$\tau_{r,1}^{(20)}$	$\tau_{r,2}^{(20)}$	$\tau_d^{(20)}$	$\tau_{d,1}^{(20)}$	$\tau_{d,2}^{(20)}$
1 mM NaCl	4	1		3.0 (34%)	12.6 (76%)		1.5 (61%)	9.4 (39%)
+ 2.5 mM		2	13.8				1.3 (59%)	7.7 (41%)
HEPES		3	21.3				1.5 (50%)	10.9 (50%)
	37	1		4.3 (73%)	23.2 (27%)	2.4		
		2		5.9 (69%)	32.0 (31%)	2.2		
		3		6.7 (63%)	27.6 (37%)	2.3		
50 mM NaCl	4	1	32.5				1.6 (33%)	9.4 (67%)
+ 2.5 mM		2		7.3 (−21%)	24 (1.21%)		1.7 (27%)	10.1 (73%)
HEPES		3	18.5				1.6 (49%)	9.0 (51%)
	37	2	18.0			2.2		
		3	15.7			2.8		

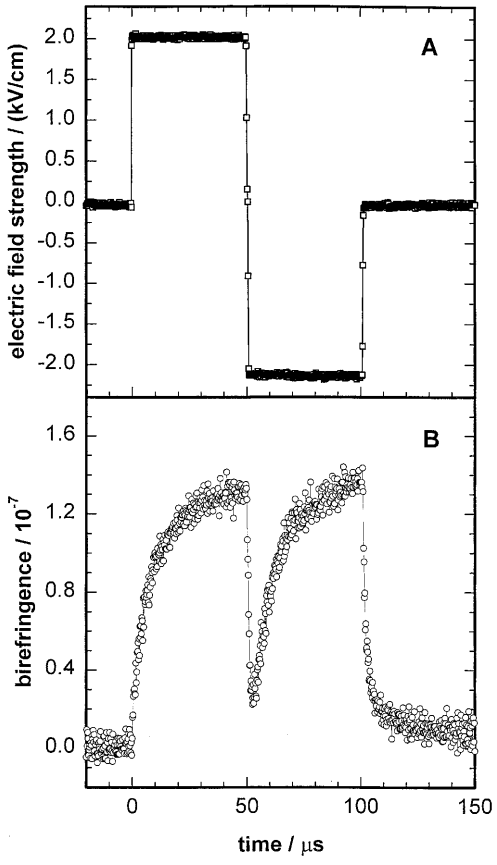

Fig. 4 **A** Symmetric, reversing electric double pulse across the Kerr cell and **B** the resulting birefringence signal of spectrin dimer (preparation 2) at 37 °C in 2.5 mM HEPES and 1 mM NaCl at pH 7.5 (○). The spectrin concentration was 0.25 mg/ml. Data points were recorded every 0.20 μs

strength solution we only observed a slightly lower value of the relative minimum. The presence of this deep minimum indicates that the permanent electric dipole moment of spectrin dimers is much larger than the induced electric dipole moment for both ionic strengths (Bjørkøy 1997; Bjørkøy et al. 1998). This is consistent with the finding that the TEB rise time is much longer than the decay time. The atomic resolution structure (Yan et al. 1993) of several of the spectrin segments and the amino acid composition (Sahr et al. 1990; Winkelmann et al. 1990) of all spectrin segments are known. The physical principles developed for predicting the permanent electric dipole moment of proteins with known structure and amino acid sequence (Davis and McCammon 1990; Antosiewicz and Porschke 1993; Antosiewicz 1995) can most likely be used to obtain reliable predictions of the spectrin segment and thus the spectrin dimer and tetramer permanent electric dipole moment. This issue will be pursued at a later time.

Assuming a spectrin dimer density of 1.37 g/ml (Kam et al. 1977), a molecular weight of 531 kDa, a hydration factor of 0.35 (Cantor and Schimmel 1980) and that the molecule is a stiff cylinder with length equal to the spectrin dimers contour length, i.e. 100 nm, we obtain an estimate of the spectrin dimer hydrodynamic diameter of about 3.5 nm. Using standard hydrodynamic theory (Tirado et al. 1984) the birefringence relaxation time of a stiff cylinder with these characteristic parameters in water is predicted to be about 16 μs at 20 °C. This predicted TEB decay is here due solely to rotational relaxation, i.e. end-over-end tumbling dynamics, of the cylinder. Because the observed time constants for dimer birefringence relaxation are much smaller than the value of a stiff rod, it can unequivocally be concluded that spectrin dimers in this case do not behave like rigid rods with length equal to the spectrin dimer contour length. The dominant observed relaxation time of 1.5 ± 0.2 μs corresponds to that of a 35–40 mm long stiff rod, but because of the complex dynamics of flexible/segmented polymer chains this does not imply that this length estimate equals the equivalent Kuhn length. The second and weaker component of the relaxation process of 9.4 ± 1 μs corresponds to that of a stiff rod with length 75–80 nm and may be associated with spectrin dimer end-over-end tumbling (rotational diffusion). Further, if the spectrin dimer was assumed to be a stiff cylinder with mainly permanent electric dipole moments in a strong electric field, the build-up time would be about three times the decay time (Fredericq and Houssier 1973), that is about 50 μs. This is significantly longer than the rise times presented in Table 1. In sum, this confirms the earlier conclusions that neither in the presence nor in the absence of an electric field does the spectrin dimer behave like a stiff molecule. The new and somewhat unexpected finding from the TEB data reported here is that the spectrin dimer intramolecular and end-over-end dynamics, as observed using TEB, appear to be virtually the same at ionic strengths 4 mM and 53 mM.

TEB of erythroid spectrin tetramers

The specific stationary birefringence $\Delta n_\infty/c$ spectrin tetramers was plotted as a function of λE^2 (data not shown) and the specific Kerr constant, B_s, was determined as shown for dimers in Fig. 2. We did not find any significant difference in the calculated values of B_s for spectrin tetramers and dimers. This is in agreement with earlier published results (Mikkelsen and Elgsaeter 1981).

Figure 5 shows a representative plot of spectrin tetramer TEB at 4 °C and ionic strength 53 mM following application of single rectangular excitation pulses. To the TEB build-up data for the solution containing 50 mM NaCl, a one-component exponential decay function can be adequately fitted, but for the solution containing 1 mM NaCl a two-component exponential decay was required. Averaged over all preparations, the time constants for the birefringence build-up were found to equal 33 μs at ionic strength 53 mM (one exponential) and 6.2 μs and 31 μs at ionic strength 4 mM (two exponentials). For the TEB decay data, a two-component exponential decay function was needed to obtain an adequately fit. Averaged over all preparations and ionic strengths the two components were found to equal 1.4 μs and 11.5 μs. Details of the results from the analyses of spectrin tetramer TEB are summar-

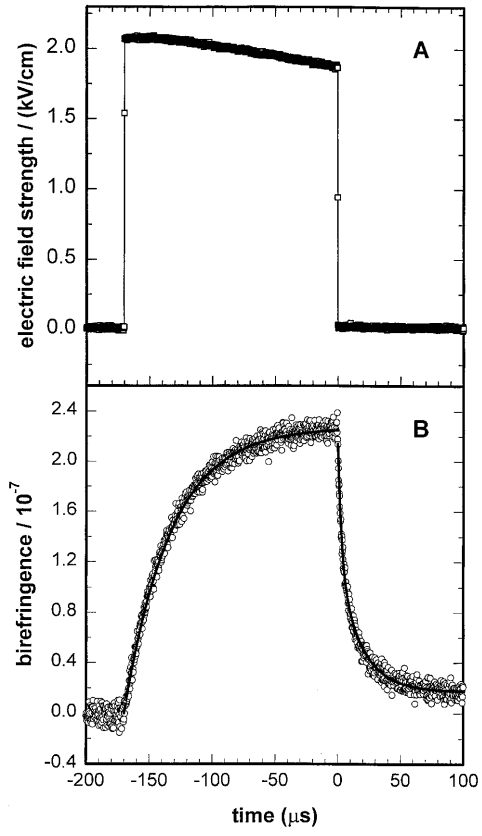

Fig. 5 **A** Electric field strength across the Kerr cell and **B** the resulting birefringence signal of spectrin tetramer at 4 °C (preparation 3) in 2.5 mM HEPES and 50 mM NaCl at pH 7.5 (○). The spectrin concentration was 0.5 mg/ml. Data points were recorded every 0.2 μs. The *solid lines* in **B** denote the best fit when a one-exponential function (build-up) or a two-exponential function (relaxation) was fitted to the experimental data using non-linear regression. The time constant for the birefringence build-up equals $\tau_r = 36.9 \pm 0.2$ μs and the two time constants for the free birefringence decay equal $\tau_{d,1} = 3.1 \pm 0.2$ μs (48%) and $\tau_{d,2} = 18.3 \pm 0.7$ μs (52%)

ized in Table 2. The values presented in Table 2 are close to earlier results on spectrin tetramer birefringence relaxation (Mikkelsen and Elgsaeter 1981; Roux and Cassoly 1982), when all data are scaled to 20 °C. The new TEB data reported here show somewhat surprisingly that the spectrin tetramer intrachain dynamic does not change significantly when the ionic strength is increased from 4 mM to about 53 mM. This probably means that the intramolecular dynamics manifesting itself in the TEB data presented also can be found at physiological conditions, i.e. when the erythrocytes are present in the bloodstream.

Figure 6 shows a representative example of the TEB when spectrin tetramers at 4 °C in 1 mM NaCl + 2.5 mM HEPES were subjected to symmetric reversing electric field pulses. The relative minimum of the birefringence after sign reversal of the electric field was found to be in the range 0.15–0.29 for 1 mM NaCl solutions and –0.09–0.01 for the 50 mM solutions. In general, the TEB is strikingly similar to that seen for dimers exposed to the same electric reversing double pulse (Fig. 4). The discussion and conclusions for dimers described above therefore also are valid for spectrin tetramers.

If the tetramers were stiff molecules consisting of two stiff dimers connected rigidly head-to-head, then the permanent dipole moments of the dimers would cancel and the total permanent dipole moment of the spectrin tetramer would equal zero. An example of this effect can be seen upon association of T-vimentin dimers to tetramers even though the association in this case is not head-to-head, but partly overlapping (Kooijman et al. 1995).

The new TEB data presented in this work show that spectrin tetramers located in an electric field have a strong permanent electric dipole moment despite the dimers making up the tetramer being connected topologically head-to-head. The most likely explanation for this is that in the presence of an electric field the flexibly linked tetramers assume a dynamic hairpin (U-shape) conformation where the permanent electric dipole moments of each of the dimers are aligned more or less parallel and in the same direction. This conformation would give rise to a dynamic structure where the permanent electric dipole moments of the two dimers do not cancel, but instead add up to give a total permanent dipole moment that is about twice that of single dimer. This is consistent with the finding that the *specific* Kerr constant is the same for spectrin dimers and tetramers.

Assuming that the spectrin tetramer molecule is a stiff cylinder with length equal to the tetramer contour length,

Table 2 Birefringence rise $\tau_r^{(20)}$ and decay $\tau_d^{(20)}$ times of erythroid spectrin tetramers obtained at 4 °C, scaled to what is predicted at 20 °C using Eq. (2). Symbols and notation are the same as in Table 1. The given time constants are the average values for electric field strengths of 0.2–1.5 kV/cm. Tetramer concentration is 0.25 mg/ml in the 1 mM NaCl buffer and 0.5 mg/ml in the 50 mM NaCl buffer. The uncertainties of the relaxation time and relative amplitude estimates are ±10%, except for the decay constant $\tau_{d,1}^{(20)}$ in the 50 mM NaCl solution and the amplitudes of $\tau_{r,1}^{(20)}$ and $\tau_{r,2}^{(20)}$, which all have uncertainties of ±15%

Ionic strength	T (°C)	Prep. no.	Time constants (μs)				
			$\tau_r^{(20)}$	$\tau_{r,1}^{(20)}$	$\tau_{r,2}^{(20)}$	$\tau_{d,1}^{(20)}$	$\tau_{d,2}^{(20)}$
1 mM NaCl	4	1		8.4 (61%)	53.6 (39%)	1.8 (58%)	14.4 (42%)
+ 2.5 mM		2		4.9 (55%)	16.1 (44%)	1.4 (62%)	9.1 (38%)
HEPES		3		5.3 (44%)	24.5 (56%)	1.4 (55%)	13.5 (45%)
50 mM NaCl	4	1	45.3			1.4 (37%)	11.7 (63%)
+ 2.5 mM		2	26.0			1.3 (41%)	10.3 (59%)
HEPES		3	27.5			1.3 (49%)	10.2 (51%)

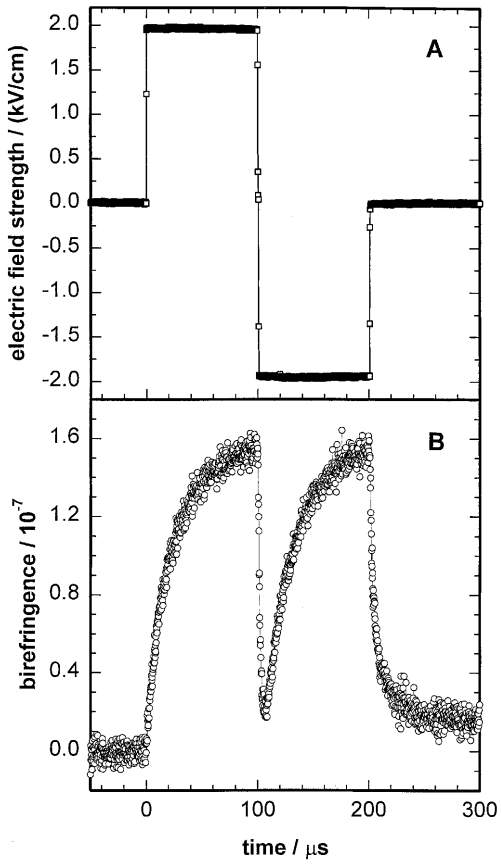

Fig. 6 **A** Symmetric, reversing electric double pulse across the Kerr cell and **B** the resulting birefringence signal of spectrin tetramer (preparation 2) at 4 °C in 2.5 mM HEPES and 1 mM NaCl at pH 7.5 (○). The spectrin concentration was 0.25 mg/ml. Data points were recorded every 0.20 μs

i.e. 200 nm, and carrying out the same calculations as above for dimers (Tirado et al. 1984), yields a predicted TEB relaxation time of about 100 μs at 20 °C. Because the longest time constant for tetramer TEB relaxation equals only about 10–15% of this value, the tetramer clearly does not undergo free end-over-end rotation as a fully extended molecule as part of the TEB experiments.

Concluding remarks

The birefringence of a solution containing rigid molecules with ellipsoidal symmetry is proportional to the amplitude of the second spherical harmonic component of angular density distribution function of the molecules (Benoit 1949; Bjørkøy et al. 1998). This is true whether the molecules are non-interacting or linked, e.g. end-to-end into long chains. This means that how the amplitude of the second spherical harmonic component of the angular distribution of all the spectrin segments changes as a result of an electric field pulse describes in full the TEB behaviour of a spectrin solution.

To calculate analytically how this second spherical harmonic component changes with time for the segmented spectrin molecule solution is not a trivial matter. One important reason for this is that the equations describing the TEB of a spectrin chain are not linear functions of the generalized coordinate describing the conformation of the spectrin chain. Non-linear dynamics can in general not be handled analytically and nothing indicates that the dynamics of the spectrin chain constitutes an exception in this regard. Because of this non-linearity it may be limited what can be extrapolated reliably from the experimental TEB data of spectrin without a detailed numerical analysis. The most obvious and maybe only feasible approach to handle this challenge is to employ Brownian dynamics simulations. Work along this line is in progress (Nyland et al. 1996; Mikkelsen et al. 1998; Skjetne and Elgsaeter 1999), but the spectrin results associated with this effort are not yet ready.

Despite the non-linearity of the spectrin dynamics a few simple points may nonetheless be semi-quantitatively discussed with some claim of reliability. The first of these is that the dynamics of a TEB experiment probably is quite different from the dynamics of, for example, a light/neutron scattering or viscometry experiment. The TEB data appear to support the notion that the spectrin tetramer in the presence of an electric field takes on an average conformation resembling that of a hairpin (U-shaped). This means that what is of importance in TEB of spectrin is:

1. The dynamics of how spectrin changes from its equilibrium conformation in a field free solution to the hairpin conformation in the presence of an electric field.
2. The dynamics of how spectrin changes from its conformation in the presence of an electric field to the equilibrium conformation in a field free solution.

In view of the suggested hairpin conformation in the presence of an electric field, it follows that the dynamics of a TEB experiment may have a quite intricate relation to, for example, nuclear magnetic resonance, light scattering or viscometry measurements. If the hairpin concept is correct, the field-free relaxation of tetramers may for example be expected to be very similar to that of a single stretched dimer relaxing to its field-free equilibrium conformation rather than that of a stretched tetramer relaxing towards the same conformation. The latter may be the reason why the TEB of spectrin dimers and tetramers somewhat surprisingly appears to be almost identical.

The new TEB data presented here provide important new experimental information about the properties of native spectrin, but quantitative analysis of the data and more detailed modelling have to await further theoretical/numerical developments.

Acknowledgements We thank the Trondheim Regional Hospital for providing outdated human blood. This work was supported by Grants no 100293/431 and 100573/410 from the Research Council of Norway.

References

Antosiewicz J (1995) Computation of the dipole moments of proteins. Biophys J 69:1344–1354

Antosiewicz J, Porschke D (1993) Brownian dynamics simulations of electrooptic transients for complex macrodipoles. J Phys Chem 97:2767–2773

Begg GE, Ralston GB, Morris MB (1994) A proton nuclear magnetic resonance study of the mobile regions of human erythroid spectrin. Biophys Chem 52:63–73

Bennett V (1990) Spectrin-based membrane skeleton: a multipotential adaptor between plasmamembrane and cytoplasm. Physiol Rev 70:1029–1065

Bennett V, Lambert S (1991) The spectrin skeleton: from red cells to brain. J Clin Invest 87:1483–1489

Benoit H (1949) Theorie de l'effet Kerr d'une solution soumise a une inpulsion electrique rectangulaire. C R Acad Sci 229:30–32

Bjørkøy A (1997) An electrooptic study of cloned spectrin segments and native spectrin. Dr.ing thesis, NTNU, Trondheim, Norway

Bjørkøy A, Elgsaeter A, Mikkelsen A (1998) Electrooptic analysis of macromolecule dipole moments using asymmetric reversing electric pulses. Biophys Chem 72:247–264

Bjørkøy A, Elgsaeter A, Mikkelsen A (1999a) Deconvolution can be used in electrooptic studies to correct for non-ideal electric excitation pulses only when the permanent dipole moment of the studied molecules is negligible. J Biochem Biophys Methods (submitted)

Bjørkøy A, Mikkelsen A, Elgsaeter A (1999b) Electric birefringence of recombinant spectrin segments 14, 14–15, 14–16 and 14–17 from *Drosophila* alpha-spectrin. Biochim Biophys Acta (in press)

Cantor CR, Schimmel PR (1980) Biophysical chemistry. Part II. Techniques for the study of biological structure and function. Freeman, San Francisco

Cole N, Ralston GB (1992) The effects of ionic strength on the self-association of human spectrin. Biochim Biophys Acta 1121: 23–30

Davis ME, McCammon JA (1990) Electrostatics in biomolecular structure and dynamics. Chem Rev 90:509–521

Dhermy D (1991) The spectrin super-family. Biol Cell 71:249–254

Elgsaeter A (1978) Human spectrin I. A classical light scattering study. Biochim Biophys Acta 536:235–244

Elgsaeter A, Mikkelsen A (1991) Shapes and shape changes in vitro in normal red cells. Biochim Biophys Acta 1071:273–290

Elgsaeter A, Shotton D, Branton D (1976) Intramembrane particle aggregation in erythrocyte ghosts. II. The influence of spectrin aggregation. Biochim Biophys Acta 426:101–122

Elgsaeter A, Stokke BT, Mikkelsen A, Branton D (1986) The molecular basis of erythrocyte shape. Science 234:1217–1223

Fredericq E, Houssier C (1973) Electric dichroism and electric birefringence. Clarendon Press, Oxford, pp 1–219

Fung LW-M, Johnson ME (1983) Multiple motions of the spectrin-actin complex in the saturation transfer EPR time domain. J Magn Reson 51:233–244

Fung LW-M, Lu H-Z, Hjelm RPJ, Johnson ME (1986) Selective detection of rapid motions in spectrin by mr. FEBS Lett 197:234–238

Goodman SR, Krebs KE, Whitfield CF, Riederer BM, Zagon IS (1988) Spectrin and related molecules. CRC Crit Rev Biochem 23:171–234

Henniker A, Ralston GB (1994) Reinvestigation of the thermodynamics of spectrin self-association. Biophys Chem 52:251–258

Kam Z, Josephs R, Eisenberg H, Gratzer WB (1977) Structural study of spectrin from human erythrocyte membranes. Biochemistry 16:5568–5572

Kooijman M, Bloemendal M, Traub P, Grondelle R van, Amerongen H van (1995) Hydrodynamic and electrical characterization of T-vimentin dimers and tetramers by transient electric birefringence measurements. J Biol Chem 270:2931–2937

Mikkelsen A, Elgsaeter A (1978) Human spectrin. II. An electro-optic study. Biochim Biophys Acta 536:245–251

Mikkelsen A, Elgsaeter A (1981) Human spectrin. V. A comparative electro-optic study of heterotetramers and heterodimers. Biochim Biophys Acta 668:74–80

Mikkelsen A, Knudsen KD, Elgsaeter A (1998) Brownian dynamics simulation of needle-spring chains. Physica A 253:66–76

Nyland GN, Skjetne P, Mikkelsen A, Elgsaeter A (1996) Brownian dynamics simulation of needle chains. J Chem Phys 105:1198–1207

Pascual J, Pfuhl M, Walther D, Saraste M, Nilges M (1997) Solution structure of the spectrin repeat: a left-handed antiparallel triple-helical coiled-coil. J Mol Biol 273:740–751

Ralston GB (1991) Temperature and pH dependence of the self-association of human spectrin. Biochemistry 30:4179–4186

Ralston GB, Dunbar JC (1979) Salt and temperature dependent conformation changes in spectrin from human erythrocyte membranes. Biochim Biophys Acta 579:20–30

Roux B, Cassoly R (1982) Differences in the electric birefringence of spectrin dimers and tetramers as shown by the fast reversing electric pulse method. Biophys Chem 16:193–198

Sahr K, Laruila P, Kotulal L, Scarpa A, Coupal E, Leta T, Linnenbach A, Winkelmann J, Speicher D, Marchesi V, Curtis P, Forget B (1990) The complete cDNA and polypeptide sequences of human erythroid alpha-spectrin. J Biol Chem 265:4435–4443

Shotton DM, Burke B, Branton D (1979) The molecular structure of human erythrocyte spectrin: biophysical and electron microscopic studies. J Mol Biol 131:303–329

Skjetne P, Elgsaeter A (1999) Implementation and performance of the needle chain-algorithm for Brownian dynamics simulation. Comput Theor Polym Sci (in press)

Skjetne P, Knudsen KD, Garcia de la Torre J, Elgsaeter A (1995) Numerical analysis of the rotational relaxation time of spectrin segments and spectrin heterodimer in dilute aqueous solution. Macromol Theory Simul 4:253–275

Speicher DW, Marchesi VT (1984) Erythrocyte spectrin is comprised of many homologous triple helical segments. Nature 311:177–180

Stokke BT, Mikkelsen A, Elgsaeter A (1985) Some viscoelastic properties of human erythrocyte spectrin networks end-linked in vitro. Biochim Biophys Acta 816:111–121

Tirado MM, Lopez Martinez C, Garcia de la Torre J (1984) Comparison of theories for translational and rotational diffusion coefficients of rod-like macromolecules. Application to short DNA fragments. J Chem Phys 81:2047–2052

Ungewickell E, Gratzer W (1978) Self-association of human spectrin. Eur J Biochem 88:379–385

Winkelmann JC, Chang J-G, Tse WT, Scarpa AL, Marchesi VT, Forget BG (1990) Full-length sequence of the cDNA for human erythroid β-spectrin. J Biol Chem 265:11827–11832

Yan Y, Winograd E, Viel A, Cronin T, Harrison SC (1993) Crystal structure of the repetitive segments of spectrin. Science 262: 2027–2030